

Designing an anisotropic noise filter for measuring critical dimension and line edge roughness from scanning electron microscope images

Hyesung Ji, and Soo-Young Lee

Citation: *Journal of Vacuum Science & Technology B* **36**, 06JA06 (2018); doi: 10.1116/1.5048077

View online: <https://doi.org/10.1116/1.5048077>

View Table of Contents: <http://avs.scitation.org/toc/jvb/36/6>

Published by the [American Vacuum Society](#)

HIDEN
ANALYTICAL

Contact Hiden Analytical for further details:
W www.HidenAnalytical.com
E info@hiden.co.uk

CLICK TO VIEW our product catalogue



Instruments for Advanced Science



Gas Analysis

- dynamic measurement of reaction gas streams
- catalysis and thermal analysis
- molecular beam studies
- dissolved species probes
- fermentation, environmental and ecological studies



Surface Science

- UHV-TPD
- SIMS
- end point detection in ion beam etch
- elemental imaging - surface mapping



Plasma Diagnostics

- plasma source characterization
- etch and deposition process reaction kinetic studies
- analysis of neutral and radical species



Vacuum Analysis

- partial pressure measurement and control of process gases
- reactive sputter process control
- vacuum diagnostics
- vacuum coating process monitoring

Designing an anisotropic noise filter for measuring critical dimension and line edge roughness from scanning electron microscope images

Hyesung Ji and Soo-Young Lee^{a)}

Department of Electrical and Computer Engineering, Auburn University, Auburn, Alabama 36849

(Received 11 July 2018; accepted 14 November 2018; published 3 December 2018)

The scanning electron microscope (SEM) is often employed in inspecting patterns transferred through a lithographic process. A typical inspection is to measure the critical dimension (CD) and line edge roughness (LER) of each feature in a transferred pattern. Such inspection may be done by utilizing image processing techniques to detect the boundaries of a feature. Since SEM images tend to include a substantial level of noise, a proper reduction of noise is essential before the subsequent process of edge detection. In a previous study, a method of designing an isotropic Gaussian filter adaptive to the noise level was developed. However, its performance for relatively small features was not so good as for large features, especially in the case of LER. The main objective of this study is to improve the design method such that the accuracy of the measured CD and LER is not deteriorated substantially as the feature size decreases. The new design method allows a Gaussian filter to be anisotropic for the better adaptability to the signal and noise, both of which show a substantial level of directional correlation. The cutoff frequency for the direction normal to features is determined to include most of the signal components, and the cutoff frequency in the other direction is set to balance the signal and noise components to be included. This procedure enables a systematic and easy design of the filter. Also, the method of estimating the noise has been modified for higher accuracy. The performance of the new design method has been thoroughly analyzed using the reference images for which feature boundaries are known. It has been shown that the anisotropic filter designed by the proposed method performs better than the isotropic filter from the viewpoint of CD, LER, and power spectral density accuracy. *Published by the AVS.* <https://doi.org/10.1116/1.5048077>

I. INTRODUCTION

Semiconductor devices are fabricated by transferring the corresponding circuit patterns onto substrates using various lithographic processes.^{1–4} A circuit pattern is written on the resist layer of a substrate system and the resist is developed subsequently. It is often required to inspect the fidelity of the written pattern on the resist. An inspection method widely used is to take a scanning electron microscope (SEM) image of the written pattern and analyze it to measure certain metrics such as the critical dimension (CD) and line edge roughness (LER) of a circuit feature. One of the analysis procedures is to employ image processing techniques by which the boundaries of features are detected and compute the CD and LER from the boundaries.^{5–14} Since SEM images tend to be noisy, it is essential to reduce the noise level before the boundary (edge) detection is carried out. The noise filtering has a direct effect on the accuracy of boundary detection, and therefore, it is critical to employ a noise filter optimized for the detection of feature boundaries in SEM images.⁶ One of the characteristics specific to typical SEM images, which may be taken into account in designing a noise filter, is that features in a circuit pattern tend to have a certain spatial orientation as in a line/space (L/S) pattern. The power spectral density (PSD) of the SEM image of such features shows a different distribution in the direction of orientation, compared to the direction normal to the orientation. Another

characteristic is that the noise in a SEM image exhibits a spatial correlation in the direction of beam scanning. Hence, the power spectral density of noise has a broader distribution in the corresponding direction. In addition, the power spectral densities of features and noise vary with the SEM image. The specific problem studied in this research is how to design a noise filter which exploits these characteristics in order to enable detecting feature boundaries accurately.

A fixed filter, e.g., median or spatial averaging filter, may be considered⁵ but would not be able to consider the above-mentioned characteristics properly. In a recent study,⁶ a method of designing an isotropic Gaussian filter of which the cutoff frequency and size are adaptively determined based on the power spectra of signal and noise in a given SEM image was proposed and tested with L/S patterns. A requirement in this design is that the signal and noise powers passed through the filter are equalized. The rationale behind the requirement is to include the high frequencies (image detail) as much as possible, especially for the accurate measurement of LER, without allowing the noise power exceeding the signal power in the filtered SEM image. The performance of the filter has been tested for several images with spatially correlated noise. Though the filter works well for relatively large features, its performance is significantly degraded in the LER measurement for small features. A possible reason is that it is an isotropic filter, while features and noise in a SEM image are anisotropic. In another study,¹⁵ the brightness distribution over a feature boundary is fitted to a (edge) model function. While its effectiveness has been

^{a)}Electronic mail: leesooy@eng.auburn.edu

demonstrated with a Gaussian function being the model function, it should be pointed out that the method would be sensitive to the shape of the brightness distribution which is likely to vary substantially with edge.

In this study, the Gaussian filter is allowed to be anisotropic to exploit the fact that both signal and noise exhibit directional dependencies in their spectra. The main objective is to develop a new method to design an anisotropic filter which works well for not only large but also small features in the analysis of SEM images. The cutoff frequencies in the horizontal and vertical directions are determined utilizing the information extracted from the signal and noise spectra of a given SEM image. The cutoff frequency in the horizontal direction, to which line features are normal, is set first by including a sufficient amount of signal power. Then, the cutoff frequency in the other direction is determined such that the noise power in the filtered image does not exceed the signal power. With a set of reference images for which feature boundaries are known, the performance of an anisotropic Gaussian filter designed by the new method has been demonstrated to be significantly better than that of an isotropic Gaussian filter in terms of the accuracy of CD, LER, and PSD (of feature boundaries).

The remainder of this paper is organized as follows. The noise estimation method is depicted in Sec. II. The new method of designing an anisotropic Gaussian filter is described in Sec. III. The results from an extensive performance analysis of the filter designed by the new method are discussed in Sec. IV. A summary is provided in Sec. V.

II. NOISE ESTIMATION

In designing a noise filter which is to be adaptive to the noise in a given SEM image, the noise estimation is an inevitable step. The estimation of noise is done in a similar way as in the previous study.⁶ A typical SEM image of the L/S pattern includes flat regions between the white regions (edge regions), within which the local average of brightness does not vary spatially. The flat regions are extracted and the DC component of brightness (the average brightness) in each flat region is removed. The flat regions are vertical strips when line features are vertically oriented as shown in Fig. 1.

The flat regions are combined together (concatenated) to form a noise image to be used as a noise estimate. In this process, the width of the flat region to be extracted is to be determined. While the width of the flat region was set manually in the previous study,⁶ it is determined through an automated procedure in this study. The noise in the SEM image is reduced by a Gaussian filter, and then the filtered SEM image is averaged along the length dimension of lines to result in a 1D brightness distribution along the horizontal dimension (see Fig. 2).

Each flat region is determined from this 1D brightness distribution. The brightness distribution of the white region gets blurred through the filtering and averaging such that the apparent width of the flat region in the 1D brightness distribution is narrower than the actual width [see Fig. 3(a)].

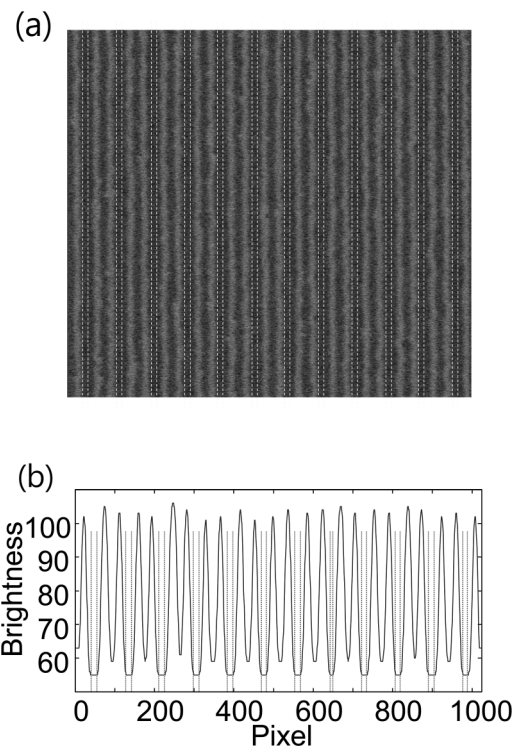


FIG. 1. (a) Flat regions are extracted from the SEM image and (b) the brightness distribution along a cross section of the SEM image (regions between dashed lines are flat regions).

Therefore, in order to maximize the width of the flat region to be extracted, the flat region is allowed to include certain regions with a small nonzero slope of brightness distribution [see Fig. 3(b)]. The threshold on the slope may be set to be a certain percent of the maximum brightness gradient in the edge (white) region. Note that the smaller the maximum gradient is, the larger the width of the nonzero slope region included in the flat region would be (if the same absolute threshold of slope is applied). The threshold may need to be adjusted depending on the maximum gradient; however, it turns out that 10% of the maximum gradient works well for the reference images considered in this study.

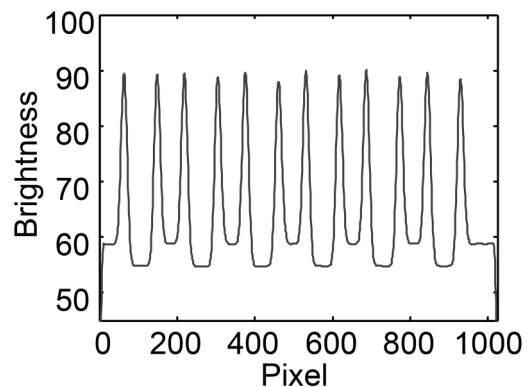


FIG. 2. Brightness distribution along the direction normal to line features after Gaussian filtering.

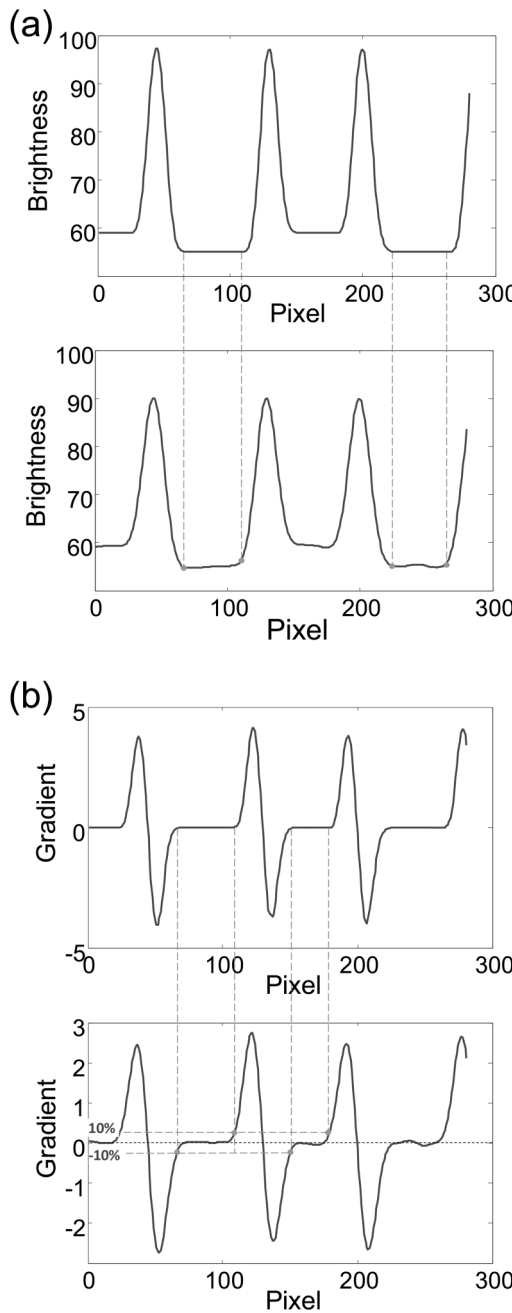


FIG. 3. (a) Brightness distribution before (top) and after (bottom) the filtering and (b) the gradient of the brightness distribution before (top) and after (bottom) the filtering.

The size of estimated noise is normally smaller than that of the corresponding SEM image since the nonflat regions are not included. Therefore, for the spectral analysis, the Fourier transform of the estimated noise needs to be scaled by a factor of $\sqrt{\frac{K}{M}}$ where the size of the SEM image is $K \times K$ and that of the estimated noise is $K \times M$.⁶ Let the Fourier transform of the estimated noise be denoted by $N_e(u, v)$ and that after the scaling by $N(u, v)$. Then,

$$|N(u, v)| = \sqrt{\frac{K}{M}}|N_e(u, v)|. \quad (1)$$

III. FILTER DESIGN

In a previous study,⁶ a method of designing an isotropic Gaussian filter to be used in reducing the noise in SEM images was proposed. A drawback observed is that the LER error is significant when the feature size is relatively small. A possible reason for the drawback is that an isotropic filter is employed though the signal and noise spectra exhibit a clear directional dependency as can be seen in Fig. 4. Hence, in this study, a new method of filter design, which takes into account the directional dependency and allows the Gaussian filter to be anisotropic, is developed.

The Gaussian filter is selected in this study due to its useful properties. The degree of filtering by a Gaussian filter can be easily controlled through its parameter of standard deviation. This property is desirable when designing an adaptive noise filter. Also, its frequency domain representation is readily derived and has the same form of Gaussian. This must facilitate the process of filter design. That is, a filter may be designed in the frequency domain and then the spatial domain representation can be easily obtained.

A. Determination of cutoff frequency

Designing a filter involves the determination of the shape and size of the filter. In the case of an anisotropic Gaussian filter, the shape is specified by the standard deviations

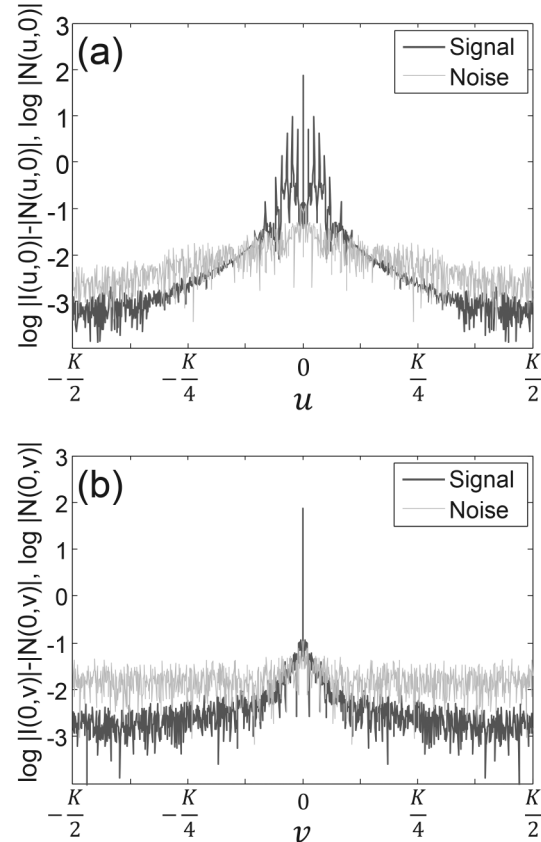


FIG. 4. (a) Signal and noise spectra along the direction perpendicular to lines and (b) the signal and noise spectra along the direction parallel with lines. $K = 1024$.

(σ_x, σ_y) in the X and Y dimensions in the spatial domain or equivalently the cutoff frequencies (σ_u, σ_v) in the u and v dimensions in the frequency domain where u and v are the frequencies corresponding to X and Y , respectively. The cutoff frequencies are determined in two steps. Noting that most of the signal power in a L/S pattern is distributed along the u -axis (when lines are normal to the X-axis), the cutoff frequency σ_u is determined first. Let $I(u, v)$ and $N(u, v)$ be the Fourier transforms of the SEM image and estimated noise, respectively. The (absolute) signal spectrum, $S(u, v)$, is defined to be $|I(u, v)| - |N(u, v)|$ in the domain where $|I(u, v)| \geq |N(u, v)|$ and 0 elsewhere. Then, the cutoff frequency σ_u is derived by finding the smallest σ_u satisfying

$$\sum_{u=-\sigma_u}^{\sigma_u} S(u, 0) \geq 0.95 \sum_{u=-(K/2)+1}^{K/2} S(u, 0), \quad (2)$$

where K is the size of the image and noise.

That is, the cutoff frequency σ_u is set such that 95% of the signal power on the u -axis is included to avoid the edge blurring as much as possible by keeping most of the signal without including too much noise. The noise is not explicitly considered in the determination of σ_u in this step. The cutoff frequency σ_v is determined in a similar way as in the previous study but with σ_u fixed. Let $G(u, v; \sigma_u)$ denote the Gaussian filter in the frequency domain, in which the standard deviation of a Gaussian filter along the u dimension is set to σ_u . Using $G(u, v; \sigma_u)$, the standard deviation along the v dimension is found such that the signal power is not less than the noise power after the filtering, i.e., the maximum frequency of v for which the ratio defined below is not less than 1.⁶ Then, the σ_u is set to the maximum frequency [see Eq. (3)].

$$\frac{\sum_{v=0}^{K-1} \sum_{u=0}^{K-1} |I(u, v)| G(u, v; \sigma_u) - \sum_{v=0}^{K-1} \sum_{u=0}^{K-1} |N(u, v)| G(u, v; \sigma_u)}{\sum_{v=0}^{K-1} \sum_{u=0}^{K-1} |N(u, v)| G(u, v; \sigma_u)} \quad (3)$$

The idea is to determine the σ_u by including most of the frequency components of line features in a L/S pattern and then the σ_v by including as much signal power as possible without allowing more noise power than the signal power. That is, the σ_u is determined mainly by the features while the σ_v is influenced more by the noise. In Fig. 5, a filtered SEM image is compared with the SEM image before the filtering. It can be seen that feature boundaries are mostly maintained while the noise level is significantly reduced.

The standard deviations, σ_x and σ_y , of a 2D Gaussian filter are related to the cutoff frequencies, σ_u and σ_v , as follows: $\sigma_x = K/2\pi\sigma_u$ and $\sigma_y = K/2\pi\sigma_v$.⁶ Then, the size of a Gaussian filter, $W_x \times W_y$, is set such that most of the significant filter coefficients are included, i.e., $W_x = 6\sigma_x$ and $W_y = 6\sigma_y$.

B. Boundary detection

After the noise filtering, the detection of feature boundaries is carried out using an edge detector. As in the previous study,⁶ the Sobel operator is employed. Since line features

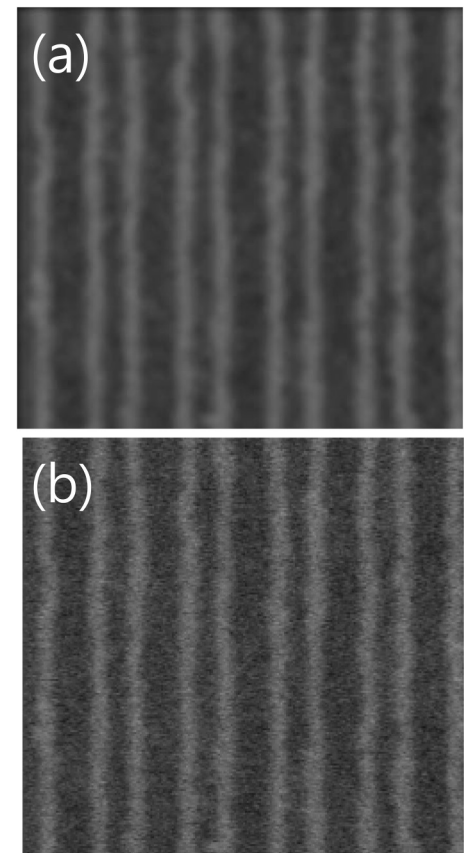


FIG. 5. Example of the magnified SEM image: (a) after and (b) before filtering.

are assumed to be oriented vertically, the vertical Sobel operator is applied to the filter SEM image. Then, the pixels with the maximum and minimum gradients within the edge region are identified to be boundary or edge pixels. In Fig. 6, a result of boundary detection is shown.

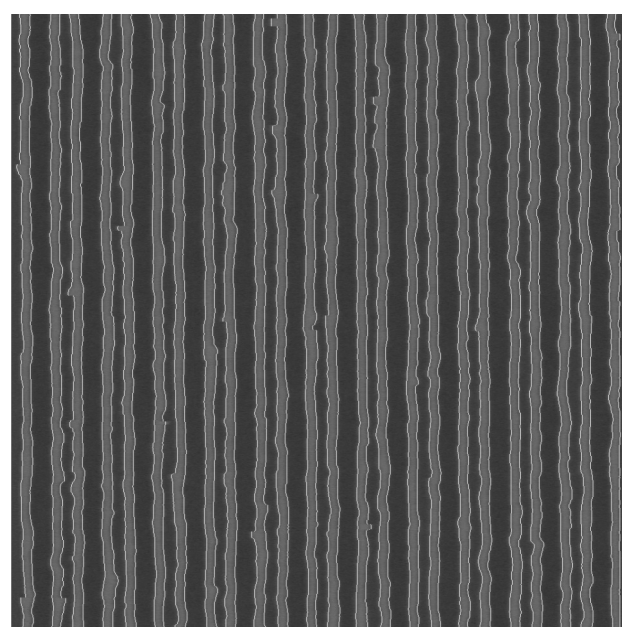


FIG. 6. Detected edges are overlaid with the corresponding SEM image.

IV. RESULTS AND DISCUSSION

The performance of the anisotropic Gaussian designed by the proposed method has been analyzed through an extensive simulation.

A. Reference image

A set of reference images for which feature boundaries (and therefore the CD and LER) are known is used for the performance analysis. Note that the true CD and LER are not known for SEM images. In order to obtain realistic reference images, most of them are generated from several real SEM images of L/S patterns as follows (refer to Fig. 7). First, from each SEM image, the inner and outer edges of each line boundary are detected. The region between the inner and outer edges is referred to as edge region. Second, a region-wise-uniform image consisting of line, space, and edge regions is constructed by setting the grayscale level of each region to the average brightness level of the corresponding region in the SEM image. Third, edge regions are smoothed in the direction normal to lines such that the shape of the brightness distribution over the edge region is similar with that in the SEM image. Fourth, a certain level/type of noise is added to the smoothed image in order to obtain a reference image.

In order to consider relatively larger LER, a small number of reference images are also created by randomly setting edge points around a straight boundary. In a previous study,^{14,16} a sophisticated technique involving the correlation length and roughness exponent was used. In this study, a simple method is employed, i.e., the magnitude and spatial variation of roughness are determined by controlling the range and sign change of random number. The rest of the procedures is the same as the last three steps above.

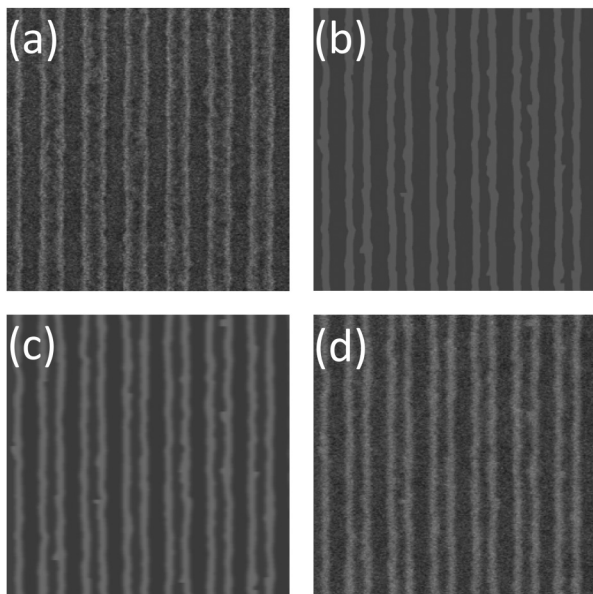


Fig. 7. Procedures of generating reference images: (a) SEM image, (b) region-wise-uniform image, (c) edge-smoothed image, and (d) noise-added image, i.e., reference image.

The added noise is generated so that it can have no spatial correlation or a spatial correlation in one or both of horizontal and vertical directions. A spatially correlated noise is obtained from a spatially uncorrelated noise through spatial interpolation where the interpolation interval determines the level of correlation. A set of basis noise instances with several different spatial correlations is generated. By combining the basis noise instances with adjustable weights, a noise instance of which the spectrum (power spectral density) is similar to that of the noise from the real SEM image is generated.

The actual CD (the width of line in a L/S pattern) in the transferred pattern may be different from the target CD depending on the dose used in the pattern transfer and also due to the proximity effect. Since the reference images are generated from the SEM images of transferred patterns, the linewidth in a reference image can be different from the target linewidth. The three target linewidths considered in this study are 50, 60, and 120 nm. The CDs and LERs in the reference images are listed in Table I.

Each reference image is filtered by the Gaussian filter designed by the proposed design method. The feature (line) boundaries are detected using the Sobel operator from the filtered reference image. Then, the CD and LER computed from the detected feature boundaries are compared to the known CD and LER to quantify the CD and LER errors. In each case, the errors are averaged over 10 simulations (noise samples). Since the CD error is much smaller than the LER error and is less than 1% in all cases, the discussion will be mainly focused on the LER error.

B. Comparison with the previous results

In this section, the results achieved by the new design method developed in this study are compared with those by the previous design method. Since the isotropic filter of the previous study did not perform well for the small features (60 nm), the comparison is made for the linewidth of 60 nm only. In Table II, the CD and LER errors for the previous and new design methods are provided. It is clear that the anisotropic Gaussian filter designed by the new design method performs significantly better than the isotropic Gaussian filter from the previous study.

C. Comparison between isotropic and anisotropic

In the remainder of this paper, the isotropic filter refers to an isotropic filter designed by the new design method. That

TABLE I. Known LER and CD in the six reference images. The feature size refers to the target linewidth and the dose is normalized, i.e., unitless.

Feature size	120 nm	60 nm				50 nm
		Dose	Dose	Dose	Dose	
LER	4.02	2.24	2.23	2.48	2.39	2.99
CD	121.92	81.35	78.04	75.12	71.67	51.00

TABLE II. Comparison between the isotropic filter designed by the previous method and the anisotropic filter designed by the new method for the reference images with a target linewidth of 60 nm, and horizontally and vertically correlated noise. The CD and LER errors are in percent.

Dose (normalized)	Noise level (%)	3.61		9.11		14.59		20.05	
		Filter type	Old-iso	Aniso	Old-iso	Aniso	Old-iso	Aniso	Old-iso
1.082	LER error	-13.66	-4.93	-14.78	-1.81	-15.15	-1.11	-14.71	-3.92
	CD error	-0.69	-0.27	-1.03	-0.28	-1.70	-0.35	-2.69	-0.37
1.000	LER error	-16.83	-4.93	-18.38	0.48	-20.32	-1.89	-20.58	-1.10
	CD error	-0.30	-0.14	-0.54	-0.13	-1.02	-0.12	-1.76	-0.14
0.92	LER error	-11.41	-6.67	-14.01	-5.78	-18.52	-3.18	-21.17	-4.53
	CD error	-0.17	-0.18	-0.17	-0.16	-0.37	-0.15	-0.81	-0.16
0.845	LER error	-7.44	-4.56	-8.21	-0.63	-11.61	4.10	-15.74	5.61
	CD error	-0.26	-0.26	-0.22	-0.22	-0.31	-0.21	-0.75	-0.24

is, the main focus of discussion will be on the comparison between an isotropic filter and an anisotropic filter (not between the previous and new results).

1. Noise with both directional correlations

The results for a set of reference images, where the noise with the same spatial correlation as in the (real) SEM images is included, are provided in Table III. The noise in the SEM images has a stronger spatial correlation in the horizontal direction than in the vertical direction, i.e., anisotropic. It can be seen that the CD and LER errors for the anisotropic (Gaussian) filter are smaller than those for the isotropic filter. The improvement achieved by the anisotropic filter tends to be larger for a higher level of noise. This may be understood by noting that the spatial correlation of noise can have a larger effect on the noise filtering when the noise level is higher. Another observation that can be made is that σ_x of anisotropic filter does not vary (increase) as much as σ_y with the noise level. In the

proposed method of filter design, the noise level affects σ_v more than σ_u (refer to Sec. III). One exception is that the anisotropic filter leads to larger CD and LER errors compared to the isotropic filter in the case of the reference image obtained from the SEM image of the L/S pattern transferred with the normalized dose of 0.920. This reference image includes more-rapidly varying feature boundaries. Such boundaries are likely to be smoothed more by the anisotropic filter in the horizontal direction (determined by σ_x), leading to an underestimation of LER.

2. Noise with horizontal correlation only

A set of reference images where the noise is spatially correlated only in the horizontal direction is employed in the performance analysis. The corresponding results are provided in Table IV. The similar observations (as in the case of the noise with both directional correlations) can be made (also refer to Table V). That is, the anisotropic filter leads to the

TABLE III. Comparison between the isotropic and anisotropic filters designed by the new method for the reference images with a target linewidth of (a) 120 nm, (b) 60 nm (average errors), and (c) 50 nm, and horizontally and vertically correlated noise. The CD and LER errors are in percent, σ_x and σ_y are in nm, and W_x and W_y are in pixel. The pixel size is 1.4 nm.

Noise level (%)	3.61		9.11		14.59		20.05	
	Filter type	Isotropic	Anisotropic	Isotropic	Anisotropic	Isotropic	Anisotropic	Isotropic
(a) 120 nm								
$\sigma_x \times \sigma_y$	1.50×1.50	4.99×0.54	3.08×3.08	5.06×2.25	4.67×4.67	5.26×4.38	6.72×6.72	5.37×7.56
$W_x \times W_y$	7×7	23×3	15×15	23×11	21×21	23×19	29×29	23×33
LER error	1.42	-1.07	1.27	-0.64	-0.75	-1.16	-4.32	-4.73
CD error	-0.13	-0.04	-0.14	-0.05	0.04	0.02	0.05	-0.03
(b) 60 nm								
$\sigma_x \times \sigma_y$	1.38×1.38	4.15×0.50	2.89×2.89	4.40×2.10	4.39×4.39	4.64×4.23	5.94×5.94	4.73×7.28
$W_x \times W_y$	7×7	19×3	13×13	19×9	19×19	21×19	27×27	21×31
LER error	4.99	-5.27	7.38	-2.17	3.50	2.57	6.53	-3.79
CD error	-0.06	-0.21	-0.20	-0.20	-0.23	-0.21	-0.42	-0.23
(c) 50 nm								
$\sigma_x \times \sigma_y$	1.29×1.29	4.60×0.45	2.26×2.26	4.56×1.09	3.06×3.06	4.49×2.05	3.76×3.76	4.49×3.13
$W_x \times W_y$	7×7	21×3	11×11	21×5	15×15	21×9	17×17	21×15
LER error	3.34	-2.33	7.77	-0.80	10.11	2.73	11.45	7.34
CD error	0.06	-0.19	-0.08	-0.24	-0.12	-0.24	-0.18	-0.29

TABLE IV. Comparison between the isotropic and anisotropic filters designed by the new method for the reference images with a target linewidth of (a) 120 nm, (b) 60 nm (average errors), and (c) 50 nm, and horizontally correlated noise. The CD and LER errors are in percent, σ_x and σ_y are in nm, and W_x and W_y are in pixel. The pixel size is 1.4 nm.

Noise level (%)	3.61		9.11		14.59		20.05	
Filter type	Isotropic	Anisotropic	Isotropic	Anisotropic	Isotropic	Anisotropic	Isotropic	Anisotropic
(a) 120 nm								
$\sigma_x \times \sigma_y$	1.46×1.46	5.00×0.59	2.88×2.88	5.03×2.11	4.20×4.20	5.14×3.76	5.49×5.49	5.20×5.65
$W_x \times W_y$	7×7	23×3	13×13	23×9	19×19	23×17	25×25	23×25
LER error	1.55	-0.99	1.87	-0.67	0.37	-0.77	-1.63	-1.58
CD error	-0.14	-0.05	-0.16	-0.06	-0.10	-0.04	0.04	-0.06
(b) 60 nm								
$\sigma_x \times \sigma_y$	1.35×1.35	4.12×0.53	2.72×2.72	4.31×1.98	3.90×3.90	4.48×3.57	5.05×5.05	4.68×5.37
$W_x \times W_y$	7×7	19×3	13×13	19×9	17×17	21×17	23×23	21×23
LER error	4.39	-5.43	7.70	-2.51	5.21	2.87	4.10	3.52
CD error	-0.05	-0.21	-0.21	-0.20	-0.21	-0.20	-0.27	-0.21
(c) 50 nm								
$\sigma_x \times \sigma_y$	1.29×1.29	4.60×0.45	2.16×2.16	4.55×0.99	2.83×2.83	4.55×1.79	3.48×3.48	4.50×2.78
$W_x \times W_y$	7×7	21×3	11×11	21×5	13×13	21×9	15×15	21×13
LER error	2.88	-2.42	7.80	-0.98	10.71	1.96	12.05	6.16
CD error	0.08	-0.18	-0.12	-0.26	-0.13	-0.29	-0.19	-0.32

TABLE V. Average CD and LER errors for each target linewidth (feature size). The CD and LER errors are in percent.

Feature size (nm)	Noise with both correlations				Noise with horizontal correlation only				Noise with no spatial correlation			
	Isotropic		Anisotropic		Isotropic		Anisotropic		Isotropic		Anisotropic	
	CD error	LER error	CD error	LER error	CD error	LER error	CD error	LER error	CD error	LER error	CD error	LER error
120	0.10	1.95	0.04	1.90	0.11	1.35	0.05	1.00	0.14	2.97	0.05	0.74
60	0.23	5.60	0.21	3.45	0.18	5.35	0.21	3.58	0.16	10.14	0.21	3.73
50	0.11	8.17	0.24	3.30	0.13	8.40	0.26	2.88	0.10	6.90	0.20	1.68

TABLE VI. Comparison between the isotropic and anisotropic filters designed by the new method for the reference images with a target linewidth of (a) 120 nm, (b) 60 nm (average errors), and (c) 50 nm, and noise with no spatial correlation. The CD and LER errors are in percent, σ_x and σ_y are in nm, and W_x and W_y are in pixel. The pixel size is 1.4 nm.

Noise level (%)	3.61		9.11		14.59		20.05	
Filter type	Isotropic	Anisotropic	Isotropic	Anisotropic	Isotropic	Anisotropic	Isotropic	Anisotropic
(a) 120 nm								
$\sigma_x \times \sigma_y$	1.19×1.19	5.00×0.45	2.03×2.03	5.00×0.93	2.70×2.70	5.04×1.65	3.31×3.31	5.18×2.36
$W_x \times W_y$	7×7	23×3	9×9	23×5	13×13	23×9	15×15	23×11
LER error	1.71	-0.86	3.17	-0.98	3.48	-0.72	3.53	-0.38
CD error	-0.14	-0.04	-0.16	-0.05	-0.12	-0.05	-0.14	-0.05
(b) 60 nm								
$\sigma_x \times \sigma_y$	1.10×1.10	4.12×0.45	1.95×1.95	4.25×0.94	2.63×2.63	4.34×1.74	3.28×3.28	4.44×2.56
$W_x \times W_y$	5×5	19×3	9×9	19×5	13×13	19×9	15×15	21×11
LER error	5.44	-5.62	11.01	-4.61	12.71	-2.23	11.41	2.48
CD error	-0.05	-0.24	-0.18	-0.20	-0.20	-0.20	-0.20	-0.19
(c) 50 nm								
$\sigma_x \times \sigma_y$	1.13×1.13	4.58×0.45	1.86×1.86	4.54×0.81	2.46×2.46	4.52×1.51	2.99×2.99	4.33×2.23
$W_x \times W_y$	5×5	21×3	9×9	21×5	11×11	21×7	13×13	19×11
LER error	3.25	-2.25	7.14	-2.17	8.31	-1.25	8.90	1.07
CD error	0.08	-0.1	-0.08	-0.22	-0.11	-0.24	-0.15	-0.24

TABLE VII. Average σ_x and σ_y for each target linewidth (feature size). The σ_x and σ_y are in nm. Note that the filter size, $W_x \times W_y$, is determined by σ_x and σ_y , i.e., $W_x = 6\sigma_x$ and $W_y = 6\sigma_y$.

Feature size (nm)	Noise with both correlations				Noise with horizontal correlation only				Noise with no spatial correlation			
	Isotropic		Anisotropic		Isotropic		Anisotropic		Isotropic		Anisotropic	
	σ_x	σ_y	σ_x	σ_y	σ_x	σ_y	σ_x	σ_y	σ_x	σ_y	σ_x	σ_y
120	3.99	3.99	5.18	3.68	3.50	3.50	5.09	3.03	2.26	2.26	5.05	1.34
60	3.65	3.65	4.49	3.53	3.26	3.26	4.50	2.86	2.24	2.24	4.24	1.42
50	2.60	2.60	4.53	1.68	2.44	2.44	4.56	1.50	2.10	2.10	4.50	1.26

smaller LER error and the improvement is larger for a higher level of noise.

3. Noise with no spatial correlation

The results for the reference images with the spatially uncorrelated noise are provided in Table VI. It is noticed that the improvement by the anisotropic filter is relatively larger compared to the cases where the noise is spatially correlated. The spatially uncorrelated noise is easier to filter in general. In addition, σ_x is set mainly to include the feature frequency components sufficiently and σ_y is determined mostly by the degree of noise filtering needed. Therefore, for a reference image with a spatially uncorrelated noise, σ_y needs to be smaller while σ_x is similar with that for the case of a spatially correlated noise. Hence, the difference between σ_x and σ_y is to be larger (refer to Table VII). However, an isotropic filter has no such adaptability since σ_x must be the same as σ_y .

4. Feature size

The CD and LER errors are averaged for each feature size in each noise type in Table V. It is clear that the performance of the anisotropic filter is better in all cases and more consistently independent of the feature size and noise type. The isotropic filter leads to a significantly larger average LER error for smaller features (50 nm and 60 nm) than for a larger feature (120 nm). On the other hand, the average LER error achieved by the anisotropic filter shows only a small variation with the feature size and noise type. This is most likely due to the better adaptability of an anisotropic filter.

5. Noise level

In Table VIII, the average filter size is provided for different noise levels and types. A general tendency is that the filter size increases as the noise level increases as expected. It is also seen that the filter size tends to be smaller for the noise with no spatial correlation than for the noise with spatial correlation. This is due to the fact that the noise with spatial correlation has a broader spectrum. In Table IX, the average CD and LER errors are shown for different noise levels and feature sizes. In most cases, the LER error is larger for a higher noise level for both types of filter. However, in the case of anisotropic filter, the error is smaller for the noise level of 9.11% than for that of 3.61%. A possible explanation is that the anisotropic filter for the noise level of 3.61% does more filtering than necessary, leading to an underestimation of LER.

D. Power spectral density

The PSD of feature (line) boundaries is also considered in analyzing the effectiveness of the proposed filter design method. The PSDs of line boundaries detected using the isotropic and anisotropic filters are computed and compared to the PSD of known (reference) boundaries. The comparison results for three typical cases are provided in Fig. 8. It can be seen that the PSD of the boundaries obtained with the anisotropic filter is much closer to the PSD of reference boundaries than that with the isotropic filter. That is, the anisotropic filter designed by the proposed design method works better than the isotropic filter in terms of the PSD as well as the LER. Note that the difference (in the deviation from the reference PSD) between them is more visible in the middle and

TABLE VIII. Average σ_x and σ_y for each noise level and spatial correlation. The σ_x and σ_y are in nm. Note that the filter size, $W_x \times W_y$, is determined by σ_x and σ_y , i.e., $W_x = 6\sigma_x$ and $W_y = 6\sigma_y$.

Noise level (%)	Noise with both correlations				Noise with horizontal correlation only				Noise with no spatial correlation			
	Isotropic		Anisotropic		Isotropic		Anisotropic		Isotropic		Anisotropic	
	σ_x	σ_y	σ_x	σ_y	σ_x	σ_y	σ_x	σ_y	σ_x	σ_y	σ_x	σ_y
3.61	1.38	1.38	4.37	0.50	1.36	1.36	4.35	0.52	1.12	1.12	4.34	0.45
9.11	2.82	2.82	4.54	1.96	2.65	2.65	4.47	1.84	1.95	1.95	4.43	0.91
14.59	4.22	4.22	4.72	3.89	3.77	3.77	4.60	3.30	2.61	2.61	4.48	1.69
20.05	5.70	5.70	4.80	6.64	4.85	4.85	4.74	4.98	3.23	3.23	4.55	2.47

TABLE IX. Average CD and LER errors for each target linewidth and noise level. The CD and LER errors are in percent.

Noise level (%)	3.61				9.11				14.59				20.05			
	Isotropic		Anisotropic		Isotropic		Anisotropic		Isotropic		Anisotropic		Isotropic		Anisotropic	
	CD	LER	CD	LER	CD	LER	CD	LER	CD	LER	CD	LER	CD	LER	CD	LER
120	0.13	1.56	0.04	0.97	0.15	2.10	0.05	0.76	0.08	1.53	0.03	0.88	0.07	3.15	0.04	2.22
60	0.05	4.94	0.22	5.44	0.19	8.69	0.19	3.09	0.21	7.13	0.20	2.55	0.29	7.34	0.20	3.26
50	0.07	3.15	0.15	2.33	0.09	7.63	0.23	1.31	0.12	9.71	0.25	1.98	0.17	10.79	0.28	4.85

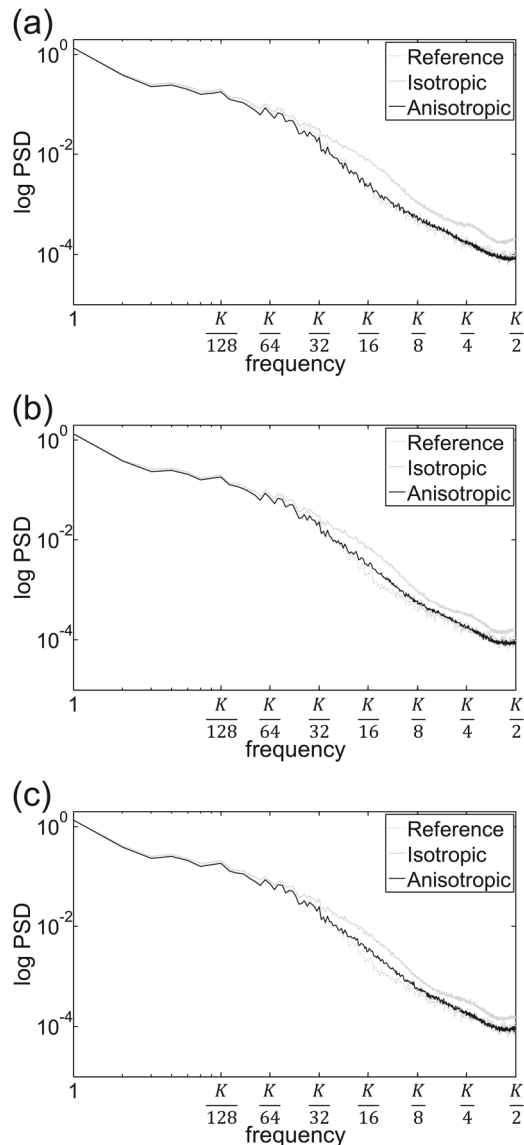


FIG. 8. Power spectral density of feature (line) boundaries when the noise has (a) no spatial correlation, (b) spatial correlation in the horizontal direction, and (c) spatial correlation in both directions. The target linewidth is 60 nm and the noise level is 9.11%. The unit of PSD is nm^2 . The frequency $K/2$ is the maximum frequency of which the period is 2 pixels where $K = 1024$ and the pixel size is 1.4 nm.

high ranges of frequency. This observation is a clear indication that the noise filtering is done better by the anisotropic filter than the isotropic filter.

V. SUMMARY

In this study, the issue of designing a noise filter to be used in the analysis of SEM images for detecting feature boundaries has been addressed with L/S patterns. The specific objective of the study is to improve the performance of a previously designed filter which is not able to achieve as high accuracy for relatively small features as for large features. The previous design method requires the same cutoff frequency in both horizontal and vertical dimensions, which leads to an isotropic filter. The new design method developed in this study allows the two cutoff frequencies to be different. The resulted filter becomes anisotropic and has a better adaptability to the noise type and level. The cutoff frequency of the filter in the direction normal to line features is first determined such that a sufficient amount of feature frequency components is included. Then, the cutoff frequency in the other direction is determined according to the degree of noise filtering needed. Also, compared to the previous method, the procedure of noise estimation has been improved in the determination of the width of the flat region to be extracted (and the DC level to be removed). Through an extensive simulation study, it has been shown that the anisotropic Gaussian filter designed by the new design method can perform better, enabling the accurate measurement of CD and LER. The CD and LER errors by the anisotropic filter are significantly smaller than those by the isotropic filter. The PSD of feature boundaries is also considered in the comparison of the filters. It is shown that the PSD by the anisotropic filter is closer to the reference PSD than that by the isotropic filter. The anisotropic filter is more adaptive to the noise type and level, and its performance is less sensitive to the feature size and noise type. Therefore, the new design method can be considered to have a potential to be employed in real applications. Nevertheless, it is worthwhile to point out that this design method relies on the noise estimated from a given SEM image. As the feature size (linewidth) decreases, the width of the flat region from

which the noise is estimated decreases, making the estimated noise less accurate. A further refinement of the noise estimation procedure may be needed. Also, another area of future study is how to set the thresholds used in estimating the noise and determining σ_u .

¹A. A. Tseng, K. Chen, C. D. Chen, and K. J. Ma, *IEEE Trans. Electron. Packaging Manuf.* **26**, 141 (2003).
²R. Murali, D. Brown, K. Martin, and J. Meindl, *J. Vac. Sci. Technol. B* **24**, 2936 (2006).
³M. J. Burek and J. R. Greer, *Nano Lett.* **10**, 69 (2010).
⁴W. Chen and H. Ahmed, *Appl. Phys. Lett.* **62**, 1499 (1993).
⁵R. Guo, S.-Y. Lee, J. Choi, S.-H. Park, I.-K. Shin, and C.-U. Jeon, *J. Vac. Sci. Technol. B* **34**, 011601 (2016).
⁶D. Li, R. Guo, S.-Y. Lee, J. Choi, S.-H. Park, S.-B. Kim, I.-K. Shin, and C.-U. Jeon, *J. Vac. Sci. Technol. B* **34**, 60K604 (2016).
⁷G. P. Patsis, V. Constantoudis, A. Tserepi, E. Gogolides, and G. Grozhev, *J. Vac. Sci. Technol. B* **21**, 1008 (2003).
⁸A. Yamaguchi and J. Yamamoto, *Proc. SPIE* **6922**, 692221 (2008).
⁹A. Hiraiwa and A. Nishida, *Proc. SPIE* **7638**, 76380N (2010).
¹⁰A. Nishida, *J. Micro/Nanolithogr. MEMS MOEMS* **9**, 041210 (2010).
¹¹A. Yamaguchi, R. Steffen, H. Kawada, and T. Iizumi, *Proc. SPIE* **6152**, 61522D (2006).
¹²A. Hiraiwa, *J. Micro/Nanolithogr. MEMS MOEMS* **10**, 023010 (2011).
¹³V. Constantoudis and E. Pargon, *Proc. SPIE* **8681**, 86812L (2013).
¹⁴V. Constantoudis, G. Papavarios, G. Lorusso, V. Rutigliani, F. Van Roey, and E. Gogolides, *J. Micro/Nanolithogr. MEMS MOEMS* **17**, 041014 (2018).
¹⁵T. Verduin, P. Kruit, and C. W. Hagen, *J. Micro/Nanolithogr. MEMS MOEMS* **13**, 033009 (2014).
¹⁶P. P. Naulleau and J. P. Cain, *J. Vac. Sci. Technol. B* **25**, 1647 (2007).